XLVI CILAMCE
VITÓRIA - ES - BRAZIL - 2025
XLVI IBERO-LATIN AMERICAN CONGRESS ON COMPUTATIONAL METHODS IN ENGENEERING

A comparative study of contact models for determining geometric properties of the wheel/rail interaction

Thiago L. Sá[1], Lucas da Silva[1], Alfredo Gay Neto[1]

[1]*Dept. of Structural and Geotechnical Engineering, University of São Paulo*
Av. Prof. Almeida Prado, 83, 05508-070, São Paulo, Brazil
t.leistersa@usp.br, lucas7.silva@usp.br, alfredo.gay@usp.br

Abstract. Creep forces are the primary mechanism for steering a wheelset on a rail track. Therefore, their evaluation is essential for modeling the train lateral dynamics, wear and rolling contact fatigue on rails and wheels. These forces are highly dependent on geometric properties such as contact position and wheel rolling radius. This study presents a comparative analysis of obtaining such contact properties using three different 2D contact models: rigid (geometric) contact, elastic penalty contact and elastic barrier contact. The case study is a scenario of a wheelset with new wheels in contact with a track with new rails. The three contact formulations yielded similar results for the wheel rolling radius, except for the regions of contact discontinuity and flange contact.

Keywords: Contact Mechanics, Wheel/rail interaction, Contact models.

1 Introduction

The accurate evaluation of contact normal and tangential forces is fundamental for studying rail vehicle dynamics according to Shabana [1]. These forces allow the wheelset to follow the track, but they can also cause dynamic instability, known as hunting, and derailment. The tangential force, called creep forces, arises from the normalized relative velocities of wheel and rail at the contact point called creepages. This relative motion is due to the difference in the wheels rolling radius, both rigidly connected to the same axle, to the wheelset's angle of attack relative to the track, and to the contact angle relative to the wheelset axle.

Creep forces are sensitive to wheel rolling radius difference with small variations leading to force saturation. The accurate evaluation of rolling radius is dependent of the accurate detection of contact points at the wheels. The wheels and rails have complex shapes, with wheels having concave regions that evolve with contact wear. These complex shapes, such as the flange root of a railway wheel profile, can induce multiple contact points that may be overlooked in some approaches. Although the common normal concept is widely applied in MBD to define contact pairs, careful examination is required to discard unsuitable solutions as discussed by Lopes et al. [2], especially when dealing with concave geometries. Therefore, the goal of this study is to discuss how different contact formulations can impact the evaluation of contact properties necessary to the rail vehicle dynamic.

2 Contact models

A contact problem can be divided in two approaches: finding the contact points and calculating the contact forces. The first is a geometric problem, while the second is a mechanical one. A contact model aims to solve one or both of the problems. Rigid contact models focus on solving the geometric problem and provide a constraint between bodies that is numerically solved to find contact points, the contact forces, although, must be solved by mechanical principles. Elastic contact models focus on modeling the mechanical problem and provide the normal, and sometimes also the tangential, contact forces, while the contact points are detected by geometric relations and search algorithms. Some elastic models named penalty contact models uses the penetration between bodies to compute the contact normal forces. Other methods called barrier contact models, avoid this penetration by defining exponential repulsion forces when the bodies are too close. Penalty contact models are easier to physically justify in terms of contact mechanics, but are more difficult to compute the contact search. In other hand, barrier contact models are more difficult to justify but simplify the contact search.

Three contact models are compared in this work: a rigid geometric contact model, a linear elastic penalty contact model and a hybrid non linear barrier contact model. All these contact models are only bidimensional, i.e, the models consider the contact between curves, or planar sections of surfaces. This simplification is reasonable for railway scenarios where the wheelset has a small angle of attack.

2.1 Rigid contact

The rigid contact method employed in this work is described by Li [3] and Shevtsov [4] which are based on the work of Wang [5]. The geometric constraint imposed by this method is that the minimum vertical distance must be zero at each wheel/rail pair. Since the wheelset has three degrees of freedom: lateral position, lateral rotation and vertical position. The lateral position is prescribed, remaining only the lateral rotation to be determined, along with the contact points. Mathematically, the problem is the same as for an arbitrary vertical position, imposing that the minimum vertical distance are the same at both pairs.

The wheelset is positioned at a desired lateral position relative to the track center and at an arbitrary vertical position above the rails. The algorithm search for the minimal vertical distance at each wheel/rail pair. The vertical distance is obtained by taking a point at the rail profile, vertically projecting this point on the wheel profile and calculating the difference between them. The minimum distance at each pair is found by sampling multiple points. Thus the precision of the method is dependent on the sampling size. If the distance at each wheel/rail pair is different the wheelset is rotated to level the vertical distances. However the contact point candidates may have shifted and the process is repeated until it converges to some tolerance in the difference of minimum distances. The solution are the contact points and the wheelset lateral rotation. From the contact points, the wheel rolling radius and the contact angles are obtained geometrically from the wheel and rail profiles.

2.2 Elastic penalty contact

The penalty contact model adopted in this study was proposed by Higa et al. [6]. The model has a 2D master-master contact approach, i.e., there is no discretization of the contact surfaces besides being treated as curves. The simplification is based on describing the wheels and rails profiles by an arc spline, i.e., a G^1 continuous set of circular arcs. The fitting of wheel and rail profiles in arc splines is presented by Silva and Gay Neto [7]. The model benefits from the fact that a pair of circular arcs has an analytical solution, in most cases unique, for the contact points and their distance. The model allows multiple contact points. The model solves both the geometric and the mechanical problem. The mechanical problem considers a contact force proportional to the arcs interpenetration. The model is implemented in the in-house software GIRAFFE [8] for multibody dynamic and static simulations.

To obtain the geometric properties, a simulation is set between a wheelset and a track section in the software GIRAFFE. In a dynamic step the wheelset gravitational load is applied fixing the wheelset lateral position centered to the track. Then in a static step, the wheelset is moved to the right of the track by imposing a controlled displacement of the wheelset center point. The wheelset is brought back to the track center in a dynamic step. And again in a static step, the wheelset is moved to the left with controlled displacement. The simulation results are the wheelset coordinates, the contact points and the contact normal forces at each simulation time step. These results are postprocessed to obtain the remaining geometric properties.

2.3 Elastic barrier contact

The barrier contact model differs from the penalty contact model in its contact force law. While the later has an active force only when there is an interpenetration between the bodies, also called indentation, the former combines a strongly repulsive barrier that prevents overlaps and an elastic force. The normal force f_n is given as a function of the gap g_n, the distance between the contact points, as follows

$$f_n(g_n) = \begin{cases} 0 & \text{if } g_n \geq \bar{g}_n \\ \epsilon_1(\bar{g}_n - g_n)^{n_1} & \text{if } \bar{\bar{g}}_n \leq g_n \leq \bar{g}_n \\ \epsilon_2\, g_n^{n_2} + c_2 & \text{if } g_n < \bar{\bar{g}}_n \end{cases}, \tag{1}$$

where $\bar{g}_n$ is an activation threshold, $\bar{\bar{g}}_n$ is the barrier threshold, ϵ_1 and n_1 are parameters of the elastic force, and n_2 controls the intensity of the barrier. The parameters ϵ_2 and c_2 ensure C^1-continuity at the transition between the elastic range and the barrier range. More details on this hybrid barrier formulation can be found in this paper by Gay Neto and Wriggers [9].

The elastic force acts in the range $\bar{\bar{g}}_n \leq g_n \leq \bar{g}_n$, which is considered the "physical" range of application.

The difference $\delta = \bar{g}_n - g_n$ is analogous to the indentation in the penalty contact. The role of the barrier range is to guarantee that the contact surfaces do not intersect, which allows us to define contact points as minimizers of distance as presented by da Silva et al. [10]. For converged time steps of the simulation, the contact points do not activate the barrier, allowing a direct comparison of the two elastic models with the same force-indentation relation. However, the configurations differ due to the activation offset in the barrier model, resulting in different wheelset coordinates and contact points, and, finally, different geometric properties.

3 Case study

This case study evaluate the contact between new wheel and rails following the configuration described in the Manchester Benchmark by Shackleton and Iwnicki [11]. The wheelset is composed of two new S1002 wheel profiles with a distance of 1360 mm between flange backs. The wheel radius at taperline is 460 mm. The track is composed of two UIC60 rail profiles mounted at 1:40 cant and gauge of 1435 mm. A vertical down force of 318.825 kN was applied at the wheelset center to represent a usual heavy haul load.

3.1 Results for the rigid contact model

The wheelset lateral position was varied from -8 mm to 8 mm in increments of 0.2 mm. Figure 1 presents all the contact pairs obtained by the rigid contact model. The geometric properties, wheel rolling radius and rail contact angle, for each wheel/rail pair are shown in Fig. 2. The step changes in the properties represent a jump of the contact points over the surface of the wheel and rail. In Fig. 1 it is possible to observe three gaps in the contact lines. These gaps represents the three step changes in the properties observed in Fig. 1 close to 0, 5 and 6 mm for the wheelset lateral position.

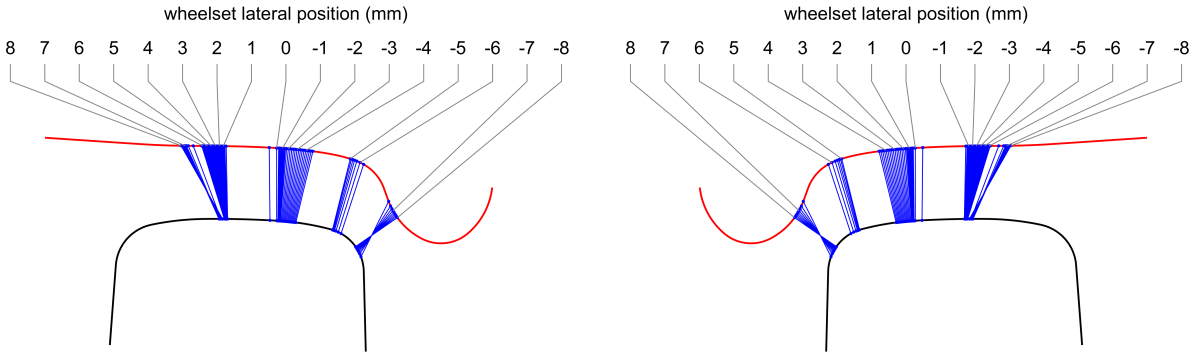


Figure 1. Distribution of contact points on wheels and rails for the rigid contact model

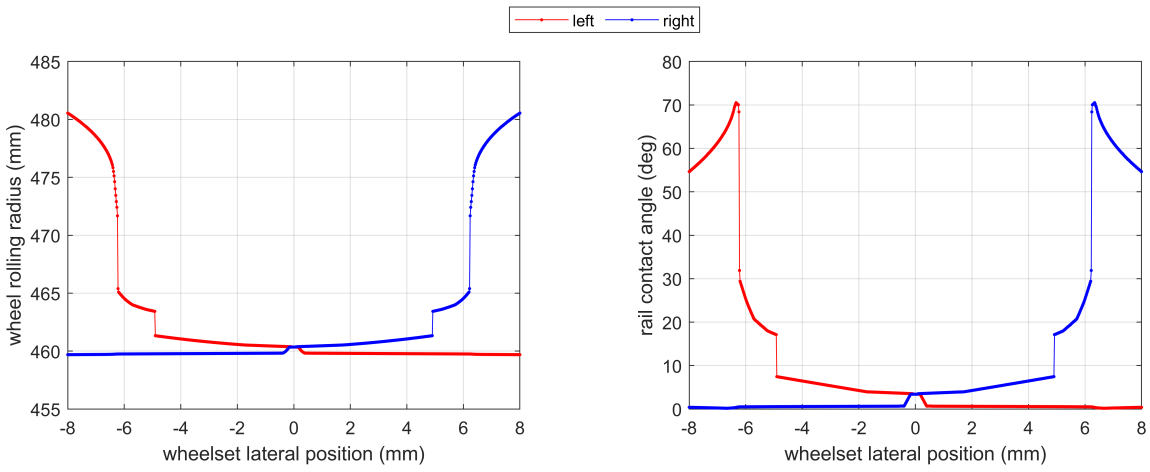


Figure 2. Rolling radius and contact angle for the rigid contact model

3.2 Results for the elastic penalty contact model

The penalty linear constant was adopted as 1×10^7 N/mm. The wheelset lateral position was varied from 0 mm to 8 mm in increments of 0.2 mm, then from 0 mm to -8 mm in decrements of -0.2 mm. The geometric properties obtained by the elastic penalty contact model are shown in Fig. 3. The mechanical simulation with controlled displacement induces the wheelset to top over when the flange contact occurs making the opposite wheel to lose contact from the rail. Thus, the results are limited to the range with contact occurring at both wheel/rail pairs. Since multiple contact points are possible for this model, the results are presented as first and second contact points defined by their normal force, with the first one the point with higher normal force magnitude.

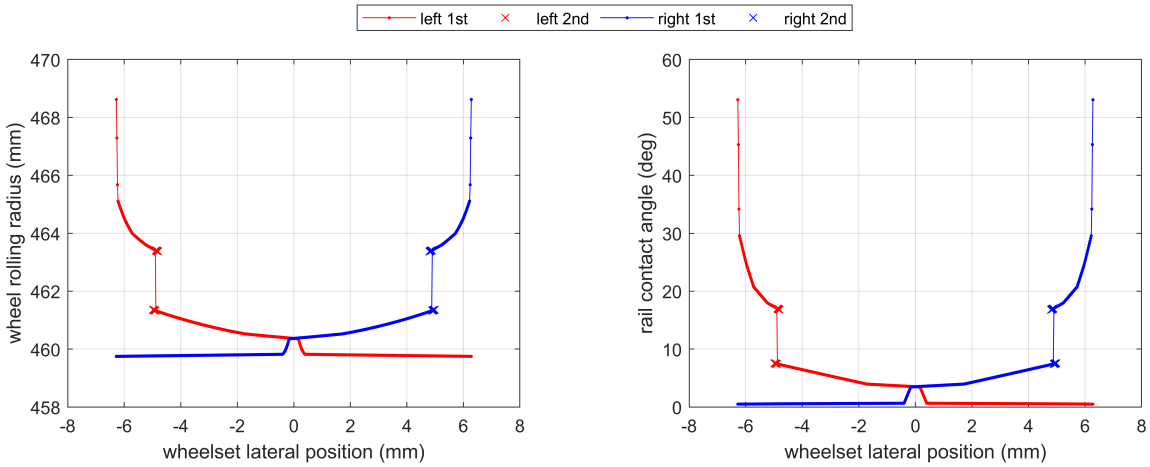


Figure 3. Rolling radius and contact angle for the elastic penalty contact model

By detecting multiple contact points, it is possible to observe that some contact jumps detected with the rigid contact model actually happens in a transition range. Figure 4 shows an enlargement of the previous plots at one of these transition zones. It can be seen that two contact points occur from 4.80 mm to 4.98 mm. The normal force at the contact points is shown in Fig. 5. The transition of the normal force from one contact point to another is clearly depicted. Figure 6 illustrates the simulation step when the contact points have similar magnitudes of normal force.

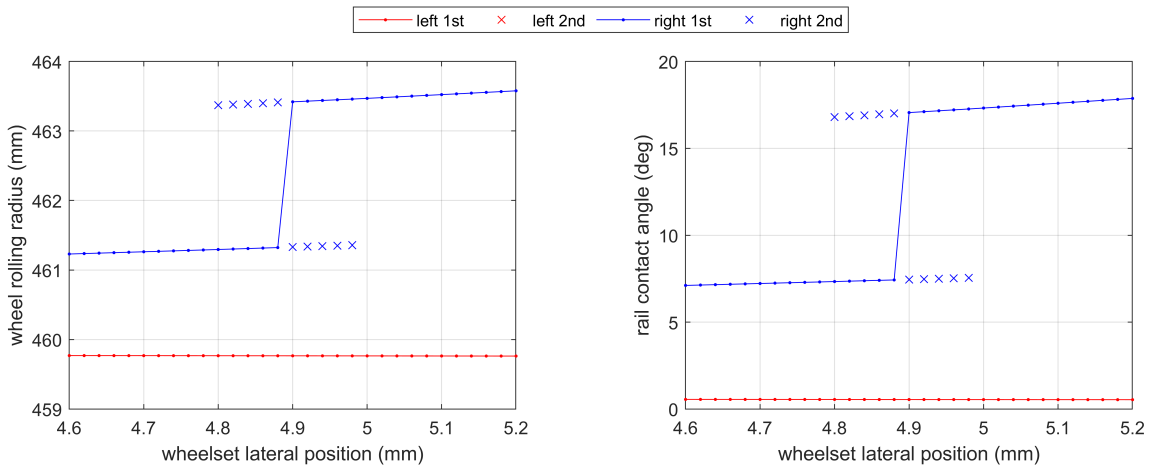


Figure 4. Enlargement of the transition zone between contact points

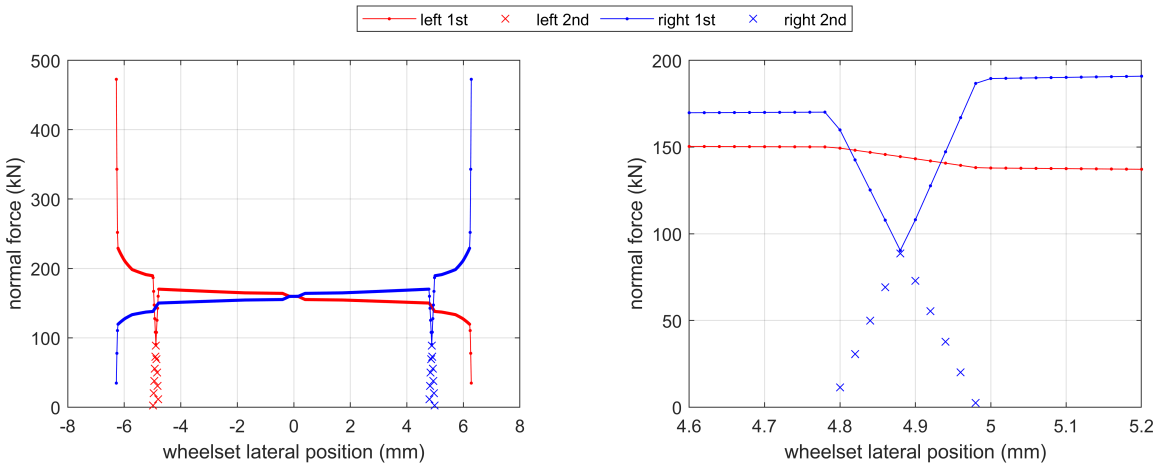


Figure 5. Normal force for the elastic penalty contact model and detail at the transition zone

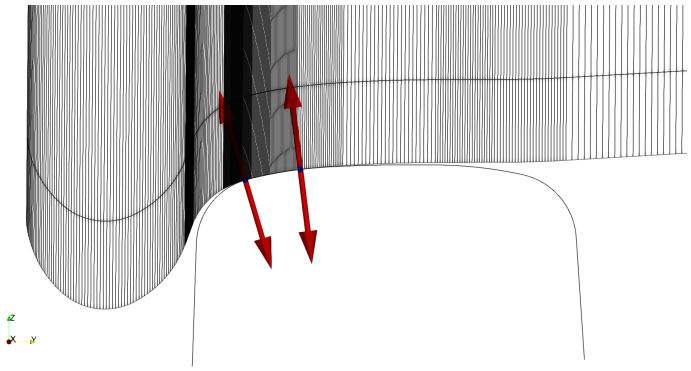


Figure 6. Double contact points for wheelset lateral position set to 4.88 mm using the penalty contact model

3.3 Results for the hybrid barrier contact model

The parameters considered for the hybrid barrier force law are $\epsilon_1 = 2 \times 10^{11}$ N/mm, $n_1 = 1$ (a linear elastic force), $\bar{g}_n = 0.1$ mm, $\bar{\bar{g}}_n = 0.001$ mm, and $n_2 = -2$. The wheelset lateral position was varied from 0 mm to 7 mm, and the results from left and right wheel were mirrored since the problem is symmetric. Figure 7 shows the wheel rolling radius and normal force obtained in the simulation. As the contact approaches the flange of the right wheel, a second contact point appears. The contact points, then, remain almost fixed while the wheelset pivots about the contact region and the contact of the left wheel is lost. The contact in this region should be conformal, since the arcs of the two profiles have equal radii. However, the offset of the barrier model makes the effective radius of the rail profile a bit larger resulting in two valid piecewise contacts at the ends of the flange root as shown in Fig. 8.

4 Discussion

All tested contact methods provided similar results for the wheel rolling radii. Figure 9 presents a direct comparison for the right wheel rolling radius. Considerable differences appear at the regions of contact jumps and the flange contact. Outside of these regions, the relative differences are lower than 0.04%.

The contact models slightly diverge between the wheelset lateral positions 4.88 mm and 4.90 mm, where there is a discontinuity in the contact. For the penalty contact model, as described earlier, there is a transition zone from 4.80 mm to 4.98 mm where the two contact points coexist. For the other two methods the contact jumps from one position to another.

At the flange contact, each formulation yielded distinctly different results. In the barrier model, a two-point contact solution is observed, while only a single flange contact point is detected by the other two methods. For the wheel and rail profiles adopted, the flange contact occurs at a region where both wheel and rail have a local radius

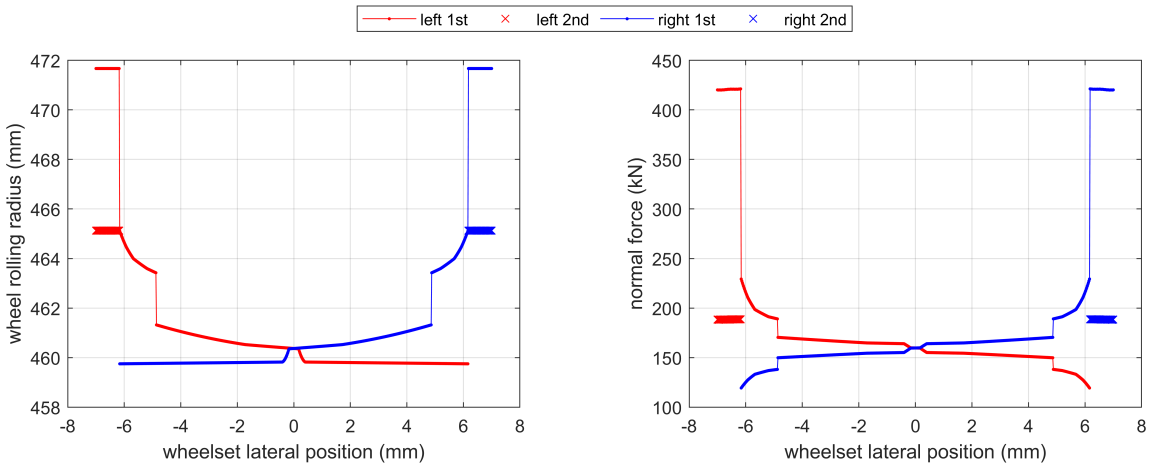


Figure 7. Rolling radius and normal force for the barrier contact model

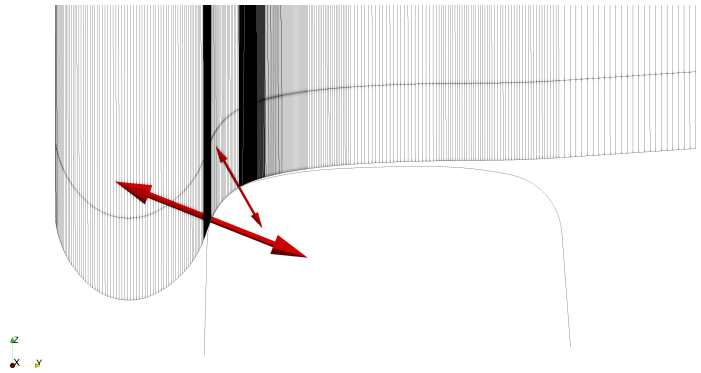


Figure 8. Double contact points for wheelset lateral position 6.18 mm using the barrier contact model

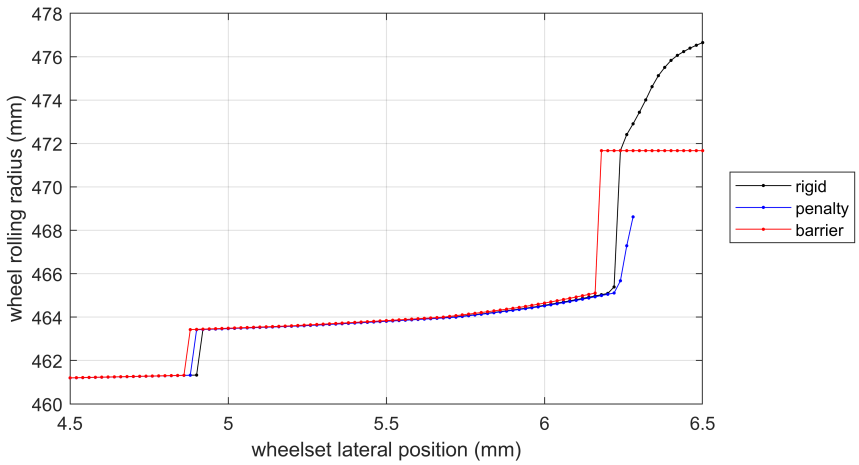


Figure 9. Comparison of the right wheel rolling radius for different contact models

of 13 mm that would lead to a conformal contact. Due to the profiles fitting procedure described earlier, the wheel flange root radius is 0.06 mm bigger than the rail gauge corner radius. This difference allows the penalty contact method to detect a single contact point. However, for the barrier method, the threshold implies the contact being detected at offset curves leading to a rail gauge corner bigger than the wheel flange root radius. This characteristic yielded to a solution with two contact points. Finally the rigid contact model, although a simpler method, was able to provide a solution in between the other two.

5 Conclusions

The elastic approaches identified configurations with more than one contact point, unlike the assumed in the rigid approach. The configurations with two contact points differ between the penalty and the barrier model. The resulting geometric properties are similar in general. A future work may study how the different flange contacts detected would influence creep force calculation and wheelset curving dynamics.

Acknowledgements. This work was financed in part by the Coordenação de Aperfeiçoamento de Pessoal de Nível Superior - Brasil (CAPES) - Finance Code 001, and supported by Vale S.A. through the Wheel-Rail Chair project. The third author acknowledges CNPq (Conselho Nacional de Desenvolvimento Científico e Tecnológico), Brazil for the financial support under the research grant 304321/2021-4.

Authorship statement. The authors hereby confirm that they are the sole liable persons responsible for the authorship of this work, and that all material that has been herein included as part of the present paper is either the property (and authorship) of the authors, or has the permission of the owners to be included here.

References

[1] A. A. Shabana. *Mathematical foundation of railroad vehicle systems: geometry and mechanics*. John Wiley & Sons, 2021.
[2] D. S. Lopes, M. T. Silva, J. A. Ambrósio, and P. Flores. A mathematical framework for rigid contact detection between quadric and superquadric surfaces. *Multibody System Dynamics*, vol. 24, n. 3, pp. 255–280, 2010.
[3] Z. Li. *Wheel-rail rolling contact and its application to wear simulation*. Phd thesis, TU Delft, 2002.
[4] I. Shevtsov. *Wheel/rail interface optimisation*. Phd thesis, TU Delft, 2008.
[5] K. Wang. The track of wheel contact points and the calculation of wheel/rail geometric contact parameters. *Journal of Southwest Jiaotong University*, vol. 1, n. 1, pp. 89–99, 1984.
[6] D. N. Higa, E. J. Kina, and A. G. Neto. Wheelset-rail mechanical model for a steady-state dynamic condition and prediction of rolling contact fatigue locci. *Vehicle System Dynamics*, vol. 60, n. 1, pp. 281–308, 2022.
[7] L. Silva and A. Gay Neto. Geometry reconstruction based on arc splines with application to wheel-rail contact simulation. *Engineering Computations*, vol. 40, n. 7-8, pp. 1889–1920, 2023.
[8] A. Gay Neto. Giraffe github repository [online] https://github.com/alfredogneto/giraffe, 2025.
[9] A. Gay Neto and P. Wriggers. Discrete element model for general polyhedra. *Computational Particle Mechanics*, vol. 9, n. 2, pp. 353–380, 2022.
[10] da L. Silva, M. V. Craveiro, and A. Gay Neto. Addressing concave boundaries in two-dimensional pointwise contact detection under the common-normal concept. *Computer Methods in Applied Mechanics and Engineering*, vol. 438, pp. 117865, 2025.
[11] P. Shackleton and S. Iwnicki. Comparison of wheel–rail contact codes for railway vehicle simulation: an introduction to the manchester contact benchmark and initial results. *Vehicle System Dynamics*, vol. 46, n. 1-2, pp. 129–149, 2008.